

University of Nebraska - Lincoln

DigitalCommons@University of Nebraska - Lincoln

---

Dissertations & Theses in Earth and Atmospheric  
Sciences

Earth and Atmospheric Sciences, Department of

---


Spring 3-24-2016

# EFFECTS OF METEOROLOGICAL CONDITIONS ON SULFUR DIOXIDE AIR POLLUTION IN THE NORTH CHINA PLAIN DURING WINTER OF 2006-2015

Chase C. Calkins

University of Nebraska - Lincoln, ccalkins@live.com

Follow this and additional works at: <http://digitalcommons.unl.edu/geoscidiss>

 Part of the [Atmospheric Sciences Commons](#), [Earth Sciences Commons](#), and the [Environmental Monitoring Commons](#)

---

Calkins, Chase C., "EFFECTS OF METEOROLOGICAL CONDITIONS ON SULFUR DIOXIDE AIR POLLUTION IN THE NORTH CHINA PLAIN DURING WINTER OF 2006-2015" (2016). *Dissertations & Theses in Earth and Atmospheric Sciences*. 77.  
<http://digitalcommons.unl.edu/geoscidiss/77>

This Article is brought to you for free and open access by the Earth and Atmospheric Sciences, Department of at DigitalCommons@University of Nebraska - Lincoln. It has been accepted for inclusion in Dissertations & Theses in Earth and Atmospheric Sciences by an authorized administrator of DigitalCommons@University of Nebraska - Lincoln.

EFFECTS OF METEOROLOGICAL CONDITIONS ON  
SULFUR DIOXIDE AIR POLLUTION IN THE NORTH CHINA  
PLAIN DURING WINTER OF 2006-2015

by

Chase Calkins

A THESIS

Presented to the Faculty of

The Graduate College at the University of Nebraska

In Partial Fulfillment of Requirements

For the Degree of Master of Science

Major: Earth and Atmospheric Sciences

Under the Supervision of Professor Jun Wang

Lincoln, Nebraska

March, 2016

# EFFECTS OF METEOROLOGICAL CONDITIONS ON SULFUR DIOXIDE AIR POLLUTION IN THE NORTH CHINA PLAIN DURING WINTER OF 2006-2015

Chase Calkins

University of Nebraska, 2016

Adviser: Jun Wang

The last decade has seen frequent occurrences of severe air pollution episodes of high concentration in SO<sub>2</sub> during winters in the North China Plain (NCP). Using satellite data from the Ozone Monitoring Instrument (OMI), chemistry transport model (GEOS-Chem) simulations, and National Center for Environmental Prediction (NCEP) meteorological reanalyzes, this study examines meteorological and synoptic conditions associated with these air pollution episodes during winters of 2006-2015. OMI-based SO<sub>2</sub> data suggest a large decrease (~30% in area average) of SO<sub>2</sub> emission since 2010. Statistical analyzes show that meteorological conditions associated with the top 10% of OMI-based high SO<sub>2</sub> days are found in average to be controlled by high pressure systems with 2 m s<sup>-1</sup> lower wind speeds, slightly warmer, 1-2 °C, temperatures and 10-20% higher relative humidities from the surface to 850 hPa. Numerical experiments with GOES-Chem nested grid simulations at 0.5°×0.667° resolution are conducted for winters of 2009 as a control year, and 2012 and 2013 as years for sensitivity analysis. The experiments reveal that year-to-year winter change of columnar SO<sub>2</sub> amount and distribution in first order is linearly proportional to the change of SO<sub>2</sub> emission, regardless of the differences in

meteorological conditions. In contrast, the surface SO<sub>2</sub> amount and distribution exhibit highly non-linear relationships with respect to the emission and stronger dependence on meteorological conditions. Longer data records of atmospheric SO<sub>2</sub> from space combined with meteorological reanalyzes are needed to further study the climatology of air pollution and the variations in air pollution events in the context of climate change.

## Acknowledgments

I would like to thank my advisor, Dr. Jun Wang, for his welcomeness, enthusiasm, encouragement, resolute dedications, financial and continued support of my program of study. I would also like to thank Dr. Mark Anderson for accepting me into the master's program and staying on my committee when I went to Jun as well as Dr. Robert Oglesby for agreeing to serve on my thesis committee and their feedback.

I would like to thank my colleagues Thomas Polivak, Xiaoguang Xu and Cui Ge for their assistance with programming, working with the chemical transport model GEOS-Chem and various satellite data sets.

I thank all of my fellow graduate students, faculty, and staff within the department for their time and support.

I would like to thank my wife, Leila, who without her help, would not have been able to complete my master's program, and to my daughter Emery, who inspires me to continue moving forward each day.

## GRANT INFORMATION

This research is funded by the work of a mini-grant sponsored by NASA-Nebraska. Any opinions, findings, and conclusions or recommendations expressed in this material are those of the author and do not necessarily reflect the views of NASA-Nebraska.

## Table of Contents

1. Introduction.....	1
2. Datasets and Study Area .....	4
2.1 OMI SO <sub>2</sub> .....	4
2.2 GEOS – Chem model .....	5
2.3 Meteorological Reanalysis Data .....	6
3. Data Processing, and Experiment Design .....	9
3.1 OMI Data Processing for Analyzing Air Pollution Meteorology.....	9
3.2 GEOS-Chem Simulation and Experiment Design .....	10
4. Results.....	11
4.1 Overview .....	11
4.2 OMI-based SO <sub>2</sub> decadal change and air pollution meteorology.....	14
4.3 Sensitivity analysis of meteorological impact on SO <sub>2</sub> .....	17
5. Summary .....	31
References.....	33

## List of tables and Figures

Figure 1. Study area.....	8
Figure 2. Background information overview.....	22
Figure 3. OMI climatology average.....	23
Figure 4. SO <sub>2</sub> mean map.....	24
Figure 5. SO <sub>2</sub> climatology map.....	25
Figure 6. SO <sub>2</sub> difference map.....	26
Figure 7. GEOS-Chem column simulation.....	27
Figure 8. GEOS-Chem surface simulation.....	28
Figure 9. Histogram of GEOS-Chem .....	29
Figure 10. Changes in winter.....	30

## 1. Introduction

Sulfur dioxide (SO<sub>2</sub>) gas is emitted both naturally and anthropogenically through volcanic eruptions and fossil fuel combustion. Estimates by the World Health Organization (WHO, 2001) show that economic health impact (excess mortality and morbidity) due to air pollution of SO<sub>2</sub> is ~43.8 billion RMB Yuan (or ~6.5 billion \$) in China. Smith et al. (2011) found that annual emissions of SO<sub>2</sub> topped ~35 Teragrams (Tg) in the US and Canada, and ~41 Tg SO<sub>2</sub> in Western and Central Europe during 1970s. However, in the last two decades, North America (United States and Canada) and Europe have been steadily reducing their emissions from 24 Tg and 31 Tg, respectively in 1990 to 17 Tg and 14 Tg, respectively in 2000, and to 15 Tg and 11 Tg, respectively in 2005. These decreasing trends contrast with the increasing trend of SO<sub>2</sub> in many developing countries; annual emissions by sector and fuel types calculated from satellite data show an increasing trend of SO<sub>2</sub> during 1996-2008 and decreasing thereafter in China, with a range of 30 – 40 Tg per year (Lu et al. 2010).

The distribution of atmospheric SO<sub>2</sub> not only depends on the emission of SO<sub>2</sub>, but also is affected by meteorological conditions. Xue et al. (2013) found that at Shanghai, SO<sub>2</sub> amounts were negatively correlated with temperature, dew point, relative humidity, wind speed and positively correlated with pressure from October 2004 to September 2012.

Bridgman et al. (2002) found that SO<sub>2</sub> concentrations in the Czech Republic can be influenced by strong variations of wind direction, wind speed and temperature within the seasons. In Trabzon City, Turkey, Cuhadaroglu and Demirei (1997) found that SO<sub>2</sub> concentrations with humidity, wind and temperature have moderate relations in



November and December while having weaker relations during January - April. However in Balıkesir, Turkey, SO<sub>2</sub> was highly correlated with lower temperatures and lower wind speeds, and less correlated with relative humidity (İlten and Selici 2008).

This study is aimed to combine a chemistry transport model (CTM), satellite products of SO<sub>2</sub>, and meteorological reanalyzes from the National Center for Environmental Prediction (NCEP) to examine how meteorological factors favor high episodes of SO<sub>2</sub> pollution events in China. Many satellite sensors have the capability to monitor atmospheric SO<sub>2</sub> from space, including the Total Ozone Mapping Spectrometer (TOMS) (Massie et al. 2004), Scanning Imaging Absorption Spectrometer for Atmospheric Chartography (SCIAMACHY) (Afe et al. 2004; Richter et al. 2006; Lee et al. 2008, 2009; Zhang et al. 2012), Ozone Monitoring Instrument (OMI) (Krotkov et al., 2008; Carn et al. 2015; Yang et al. 2007; He et al. 2012), and most recently Ozone Mapping and Profiler Suite (OMPS) (Yang et al. 2013). However, these satellite-based SO<sub>2</sub> data in the past have been primarily used for estimating the SO<sub>2</sub> emissions and to some extent to evaluate and improve CTM simulation of the atmospheric SO<sub>2</sub> (Lee et al.; 2009, 2011; Wang et al. 2013). Yang et al. (2013) is among the few studies that have combined meteorological data and satellite SO<sub>2</sub> data from OMPS, to study the role of the atmosphere in an air pollution event for winter 2013 in China. Numerous studies have also conducted ground-based observations and modeling analyses of air pollution events in China (Chan et al. 2008; Lu et al. 2010, 2011; Zhang et al. 2015), just to name a few. Our study area focuses on Northern China Plain (NCP) where the SO<sub>2</sub> emissions have changed rapidly due to the combination of fast economic growth and implementation of

air pollution control policy in this region in the last decade (Li et al. 2010). However, these rapid changes of SO<sub>2</sub> emission together with frequent SO<sub>2</sub> pollution episodes also make NCP a unique place to combine both satellite data and CTM results to study air pollution meteorology (Yang et al. 2013). Past studies of air pollution meteorology have primarily relied on the ground-based observations and numerical models (Fiore et al. 2012). Hence, our joint and new analysis of satellite and model data can reveal (to some extent) how the changing climate (including meteorological conditions) may affect SO<sub>2</sub> air quality, and thus have important implications for predicting future air quality as the climate continues to change (Fiore et al. 2012). The time period of this study is the meteorological winter (December, January and February) during 2006 - 2015. We describe the data and model in Section 2, model experiment design and approaches in Section 3, results in Section 4 and conclude the paper in Section 5.

## 2. Datasets and Study Area

Data used in this study over the NCP (110°E-125°E, 30°N-42°N, Figure 1) include: (1) Level 3 OMI-best pixel scans, (2) hourly data from GEOS-CHEM; and (3) reanalysis meteorological data from NCEP.

### 2.1 OMI SO<sub>2</sub>

The Ozone Monitoring Instrument (OMI) is a sun-synchronous polar orbiting Dutch/Finnish sensor on the AURA satellite launched on 15 July 2004. OMI is a nadir viewing imaging spectrograph that measures backscattered solar radiation over the 264-504 nm wavelength. The first UV band is from 263-311 nm while the second band is from 307-383 nm. The absorption spectrum of SO<sub>2</sub> is typically between 305-330 nm. OMI uses the 310.8-314.4 nm wavelength to capture the SO<sub>2</sub> in the atmosphere. OMI's pixel size is 13 km (along the orbit) and 24 km (across the orbit) at nadir, but can be zoomed to 13 km x 12 km to look between clouds and retrieve SO<sub>2</sub> and other aerosols. (Levelt et al. 2006). OMI's field view of 114° corresponds to a 2600 km wide swath on the surface, which enables daily global coverage. It uses a 2-D Charge Coupled Device (CCD) that can obtain spatial and spectral data simultaneously. Beginning on 25 June 2007, the OMI sensor has been flagged for row anomalies, of which, changes over time. Row anomalies are an anomaly that affects the radiance data in all wavelengths in a particular view direction. Through 28 February 2015, rows 21-54 have been affected by this anomaly which accounts for 39% of the data.

For this study, we used the planetary boundary layer (PBL) SO<sub>2</sub>\_PBL data from the level-3 OMI/AURA SO<sub>2</sub> data product, OMSO2e (Version 003) (Krotkov et al. 2010), retrieved in 2015, for the meteorological winter from 1 December 2005 to 28 February 2015. The OMI SO<sub>2</sub> product has been validated over China (Krotkov et al., 2010). The current version of OMSO2e contains the best pixel of the data. These data have been screened for OMI row anomaly and other data quality flags. During the available 900 days of data, only 870 contained data. SO<sub>2</sub> accuracy depends on two components: the uncertainty in slant column density (SCD) and the average photon path, characterized by the error in assumed air mass factor (AMF). Also, depending on vertical distribution, aerosols and sub pixel clouds affect AMF.

## *2.2 GEOS – Chem model*

The global chemical transport model GEOS-Chem (v9-01-03) is driven by the Goddard Earth Observing System (GEOS) (Bey et al. 2001) of the NASA Global Modeling and Assimilation Office (GMAO). We use GEOS-Chem for a 3-month simulation during the winter months of sulfate aerosols with a spinup of 1 month with full chemistry.

Assimilated meteorological fields from GEOS of NASA Global Modeling Assimilation Office are used to drive GEOS-Chem (Park, 2004). The model uses GEOS-5 meteorological fields with 47 vertical levels initially ran at 4° latitude by 5° longitude and then at a nested run at 0.5° latitude by 0.667° longitude. The bottom model layer is ~100 m thick above the surface. The temporal resolution is a 6h average for the 3-D meteorological variables and a 3 h average for the 2-D variables.

The global anthropogenic emissions for  $\text{NO}_x$ ,  $\text{SO}_x$ , and CO are based on the Emissions Database for Global Atmospheric Research (EDGAR) emission database (Olivier and Berdowski, 2001). The global emission is replaced by Streets 2006 emissions (Zhang et al. 2009) from the Intercontinental Chemical Transport Experiment-Phase B (INTEX-B) aircraft mission for the nested model run. The INTEX-B mission represented 22 different countries for the year 2006 with a spatial resolution of 30 minutes by 30 minutes done monthly. However, when this inventory was developed in 2006 and 2007, most of the available statistics for Chinese provinces were for the 2004 and 2005 years with the exception of a few 2006. This dataset was then extrapolated to 2006 based on various fast track statistics that were published monthly. For China, the 2006 national emission total for  $\text{SO}_2$  is  $\sim 31$  Tg/year. The convection and transport timestep of our model is set to 30 minutes and the emission timestep is set to 60 minutes for the  $4^\circ$  latitude by  $5^\circ$  longitude resolution, while the nested grid is run at 10 minutes and 20 minutes, respectively.

### *2.3 Meteorological Reanalysis Data*

The meteorological data used for studying the change of large scale dynamics and meteorological conditions are from NCEP reanalysis data, which are available from January 1948 – present. We didn't use the GEOS meteorological data to study the meteorological anomaly because of its short record that doesn't cover the time period (1981 – 2010) used in this study for computing the climatological mean of all meteorological variables. The NCEP reanalysis data are reported daily. These data are available from the daily and monthly composites from the National Oceanic and Atmospheric Administration (NOAA) Earth System Research Laboratory (ESRL) (Kalnay et al. 1996) physical science data (PSD), Boulder, Colorado, USA from their

Web site <http://www.esrl.noaa.gov/psd/>. The data variables used for this study are 850 hPa temperature, 850 hPa relative humidity, 850 hPa height, 850 hPa U and V wind vector components to make wind speed and surface pressure. The current version of the data was accessed on 13 August 2015.

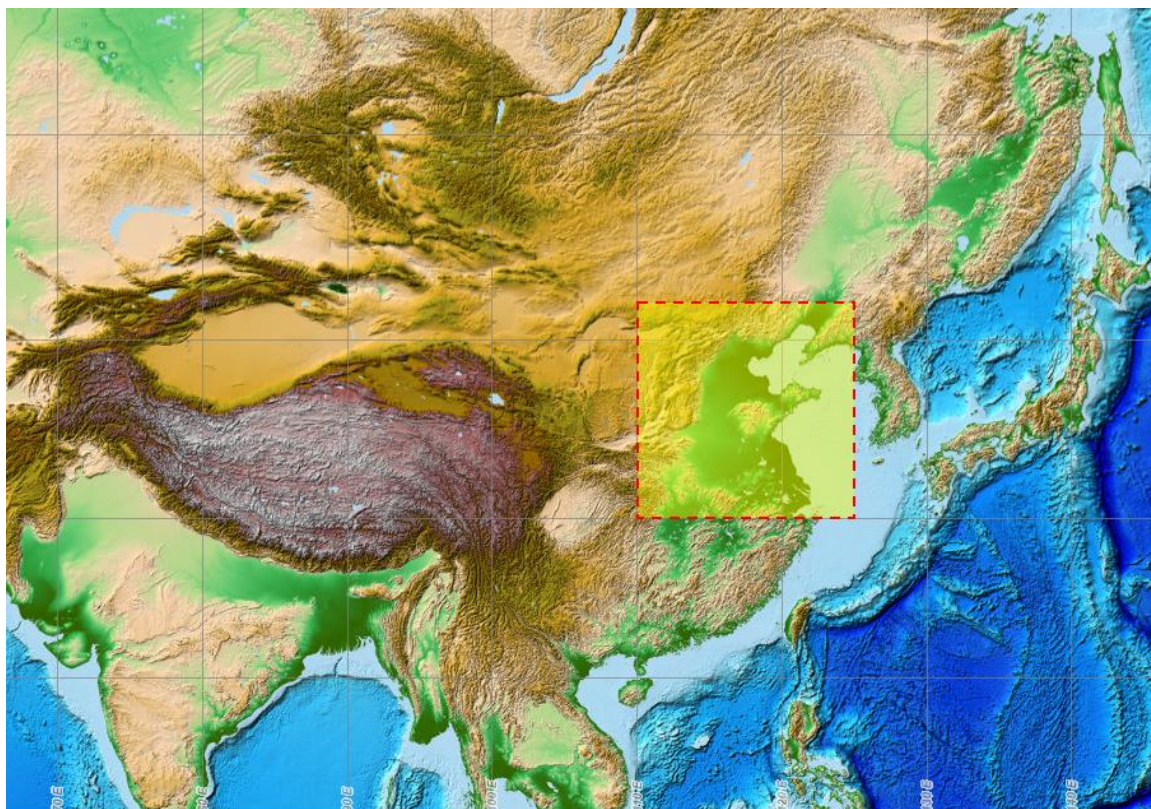


Figure 1. Highlighted area of study.

### 3. Data Processing, and Experiment Design

#### 3.1 OMI Data Processing for Analyzing Air Pollution Meteorology

Daily retrievals from OMI, allocated to grid cells of  $0.25^\circ \times 0.25^\circ$ , were filtered with a large solar zenith angle and viewing zenith angle greater than  $70^\circ$ . To further ensure data quality, only  $\text{SO}_2$  data retrieved with low radiative cloud fraction less than 0.2 are used in this study. First, we re-grid daily OMI  $\text{SO}_2$  into a  $2.5^\circ$  by  $2.5^\circ$  mesh to match the resolution of NCEP reanalyzes. Second, for each grid box, we sort the OMI  $\text{SO}_2$  data from the highest to the lowest during the winters of 2006-2015, and then index the days that have  $\text{SO}_2$  concentration in the top 10% percentile of all valid OMI  $\text{SO}_2$  data for that grid box; hereafter these days are called extreme  $\text{SO}_2$  days. Third, meteorological conditions (from NCEP) on the extreme  $\text{SO}_2$  days are averaged for each grid box; the combination of averaged parameters in each of grid boxes yields the typical meteorological conditions for high  $\text{SO}_2$  concentrations. Since  $\text{SO}_2$  concentrations are primarily located within the planetary boundary layer, we focus on the analyses of the meteorological conditions in the lower troposphere at the 850 hPa level.

To generate monthly distribution of  $\text{SO}_2$ , OMI  $\text{SO}_2$  data is also re-gridded into spatial resolution at  $0.5^\circ$  by  $0.5^\circ$  to be comparable to the resolution of GEOS-Chem nested grid resolution and also to ensure that we have enough data samples in each grid box to capture the regional scale of  $\text{SO}_2$  climatology. A minimum of five days of available  $\text{SO}_2$  data per grid box are required to compute the monthly mean of  $\text{SO}_2$  for that grid box. These monthly gridded  $\text{SO}_2$  data in first (2006-2010) and second 5 years (2011-2015) are



also added together create a map to with a minimum of seventy-five days per grid box to create 5-year averages of SO<sub>2</sub>. The decadal averages are the computed by averaging the ten years of data with a minimum of one hundred and fifty days per grid box.

### *3.2 GEOS-Chem Simulation and Experiment Design*

Various GEOS-Chem simulations are conducted to analyze the change of atmospheric SO<sub>2</sub> due to the change of emission and/or meteorological conditions. The first set of simulations is run with the same default emission for winters of 2009 (normal), 2012 (wet) and 2013 (dry year), thereby enabling the analysis of the response of atmospheric SO<sub>2</sub> to the change of meteorological conditions. The second set of simulations is the same as first set, but with emission reduced by 50%. Contrast analysis between the first and second set of simulations of the same year can reveal if the reduction of SO<sub>2</sub> emission by 50% lead to the overall decrease of atmospheric SO<sub>2</sub> by 50%, and how such decrease may change spatially? In addition, with these two sets of simulations, we can also analyze the change of SO<sub>2</sub> episode (in terms of peak of atmospheric SO<sub>2</sub> amount) due to change of emission, meteorological conditions, and combined effects.

## 4. Results

### 4.1 Overview

The NCP is flat with topography less than 100 m, (Figure 2A). However, the Taihang mountain range, located to the west of the NCP can extend higher than 1500 m. Figure 2B also shows the locations of each province in our study region. During the winter months, the climatological average (1981-2010) for the 850 hPa height ranges from 1440 geopotential meters (gpm) in northeastern part of the study region to 1530 gpm in the southwestern part, with major cities like Beijing near 1490 gpm and Shanghai near 1515 gpm (Figure 2F). Since the standard 850 hPa height is 1500 gpm, the meteorological conditions conducted over the mountains in this study have little weight in our results, because those observations would be below the surface. The precipitation climatological average during winter is relatively dry in the northern part of the plains, with Beijing receiving less than 5 mm, Shanghai around 35 mm, and the southern part of the plains receiving around 70 mm (Figure 2K).

To determine the meteorological condition patterns for high and low concentrations years, four years were investigated including; two high years, winter 2008 (Figure 2B) and winter 2012 (Figure 2D), one intermediate year, winter 2013 (Figure 2E) and one low year, winter 2009 (Figure 2C). The highest SO<sub>2</sub> concentration event came in winter 2008. Areas of high concentration are characterized by OMI values of SO<sub>2</sub> greater than 0.5 DU. There are distinct areas east of the Taihang mountain range that are continuously exceeding 0.5 DU. However, the concentrations seen in winters 2009, 2012 and 2013 are not as heavily polluted as winter 2008 concentrations, though there are similarities in

areas. There is a clear boundary of higher concentrations that forms east of the Taihang mountain range. The high SO<sub>2</sub> concentrations observed in winter 2008 can be attributed partially to higher heights at the 850 hPa level, around 10 gpm, above the climatological average (Figure 2G). Precipitation is generally near normal or slightly dryer in the same area (Figure 2L). The relatively dryer area is also where precipitation is less than 5 mm on average. Regions of higher heights and dryer conditions will generally lead to higher SO<sub>2</sub> concentrations. Winter 2009, our GEOS-Chem control year, saw lower heights, around 10 to 20 gpm (Figure 2H), and precipitation was near normal or slightly wetter (Figure 2M), leading to a decrease in SO<sub>2</sub> concentrations.

The other high concentration year, winter 2012, is similar in concentration regions observed in winter 2008. The region still sees values greater than 0.5 DU, however, winter 2012 concentrations are generally lower than those found during 2008. Winter 2013 is classified as an intermediate year, because winter 2013 concentrations are between winter 2012 and winter 2009.

In winter 2012, the 850 hPa height anomalies (Figure 2I) are similar to those of winter 2008 (Figure 2G) with the SO<sub>2</sub> concentrations being in regions of higher heights, around 10 gpm above normal. Precipitation in winter 2012 (Figure 2N) is much less compared to winter 2008 (Figure 2L), leading us to assume that winter 2012 should be as high or more severe of a concentration event than winter 2008. However, there is a significant decrease in SO<sub>2</sub> concentration over the region compared to winter 2008. The decrease was caused by January 2012 850 hPa heights, as they were near normal to 10 gpm below the climatological average and February 2008 was 20 gpm above climatology. The December months are similar to each other and cancel each other out (not shown). In

winter 2013, height anomalies (Figure 2J) are similar to winter 2009 (Figure 2H) with the concentration in an area of 10 gpm less than the climatological average. Between the two years, precipitation is the main difference. Precipitation in winter 2013 is greater, around 10 to 20 mm more than the climatological average (Figure 2O) and winter 2009 (Figure 2M) varies between -10 to 10 mm. We expect winter 2013 concentrations to look like winter 2009 or have lower SO<sub>2</sub> concentrations based the same heights and more precipitation, however, there are regions of higher concentrations. Winter 2009 is lower in concentration because February 2009 heights were 20 to 30 gpm less than the climatological average while the December and January height field canceled each other out (not shown).

Generally speaking, higher heights will lead to an increase in SO<sub>2</sub> concentrations, while lower heights will lead to lower SO<sub>2</sub> concentrations. Although precipitation plays some role in higher and lower concentrations, the major meteorological factor seems to be heights. Higher heights lead to stagnant air. This stagnant air allows for the concentration to have a longer lifetime in the region and is not able to disperse as it normally would. Winter 2012, with the same height field as winter 2008 and dryer conditions, should lead to similar or higher concentrations. However, winter 2012 concentrations were lower. Also, winter 2013, though similar in heights in winter 2009 and wetter should lead to similar concentrations observed in winter 2009. However, winter 2013 concentrations were higher. Since winters 2012 and 2013 are not what we expected when comparing them to winters 2008 and 2009, we look to explore other meteorological factors that can attribute to these high concentration events.

#### *4.2 OMI-based SO<sub>2</sub> decadal change and air pollution meteorology*

Most of eastern China's SO<sub>2</sub> concentrations are found between 112°-122°E and 34°-40°N, as observed in the 10-year winter average of OMI SO<sub>2</sub> (Figure 3A). From the decade worth of data obtained from OMI, we broke down the data into two-five year periods; (1) 2006 -2010 and (2) 2011-2015, to observe changes in SO<sub>2</sub> concentrations since the installation of flue-gas desulfurization devices in power plants. These devices have been regulated by the Chinese government since 2006. During winter of 2006-2010, (Figure 3C), the average SO<sub>2</sub> concentration was 0.77 DU with a maximum concentration of 1.76 DU for the region. For winter of 2011-2015, (Figure 3D), the average decreased to 0.55 DU (29.1% less) and the maximum concentration decreased to 1.28 DU (27.4% less). The highest local concentrations are located to the east of the Taihang Mountains along the border between Shanxi and Hebei province (Figure 3). Most of this area is around 1.0 DU during winter 2006-2010 and was reduced to around 0.7 DU during 2011-2015. We checked to see if meteorological conditions had made a significant difference during the two time periods and found the 850 hPa heights and precipitation were near climatological averages (not shown) for both time periods. Our findings are similar to those found by Lu et al. (2010), where they also found reductions to be the most significant over eastern China.

During the decade of data from OMI, we next broke down the SO<sub>2</sub> data and correlated a climatological average and the top 10% maxima of SO<sub>2</sub> data days with mean meteorological conditions. These meteorological factors include: (1) 850 hPa heights, (2) 850 hPa temperatures, (3) 850 hPa relative humidities, (4) 850 hPa wind speeds, and (5) surface pressures. We calculated a mean of the top 10% (Figure 4), climatological

average (Figure 5) and a difference between the two (Figure 6) for each grid box and contoured those results. Here we define the climatology for SO<sub>2</sub> as the 870 days of data from OMI. It should be noted that during the period, not every grid box has a data value for all 870 days, meaning, a grid box is averaged over the total number of days there are data values in that grid box and each value must be greater than 0 DU.

First, we calculate the conditions for the top 10% SO<sub>2</sub> days. The mean SO<sub>2</sub> (Figure 4A), has high concentrations around the province of Shanxi, with a maximum concentration of almost 4 DU. This region has many coal power plants that help contribute to the high maxima that we found. Surface pressures (Figure 4C) are around 1000 hPa over eastern China and decreases over the mountains to the northwest. The 850 hPa heights (Figure 4B) are around 1530 m in southern and eastern China to around 1440 m over northeastern China. 850 hPa relative humidities (Figure 4D) are mostly between 30-50%, with higher values above 50% to the northwest, because of the mountains. The 850 hPa wind speeds (Figure 4E) are between 4-10 m/s and the 850 hPa temperatures are relatively cold between -2°C and -8°C. These meteorological conditions play a major part in contributing to the high concentration top 10% SO<sub>2</sub> days. The higher heights indicate there is a stronger high pressure system over southern and eastern China. The majority of maxima SO<sub>2</sub> concentrations occur in areas of higher heights and lower wind speeds. Temperature and relative humidity are also cold and dry, meaning that we expect wet deposition to not take place, thus not allowing the removal of SO<sub>2</sub>.

Second, we calculate the climatological conditions. The climatology (Figure 5A) shows that NCP SO<sub>2</sub> concentrations are greater than 0.5 DU, with the highest concentrations greater than 1.25 DU. Our climatology of surface pressure (Figure 5C), when comparing

to the mean top 10% concentration days (Figure 4C), is nearly identical. We expected this, as surface pressures did not vary as greatly as other meteorological conditions. The climatological 850 hPa heights, (Figure 5B), are nearly identical to the 1981-2010 height climatology (Figure 2F). The 850 hPa relative humidity climatological values (Figure 5D) are slightly dryer than the top concentration days (Figure 4D), and the dryer area has shifted significantly northwestward. The 850 hPa wind speeds (Figure 5E) also show similar wind speeds to the top 10% concentration mean conditions (Figure 4E), however, lower speeds are found over where the highest area concentrations are located. Meanwhile, the 850 hPa temperature gradients, (Figure 5F), varies greatly compared to the top 10% conditions (Figure 4F).

Finally, we calculate the difference between the top 10% and the climatological conditions. The area of greatest concern for  $\text{SO}_2$  (Figure 6A), is the area greater than 0.5 DU, indicating that this area is continuously exposed to health risks using the criteria set by the WHO (2001). Our surface pressure differences (Figure 6C) show no indication of having any impact on  $\text{SO}_2$ . Our 850 hPa height differences, (Figure 6B), show that areas of higher heights will lead to higher concentrations in  $\text{SO}_2$ . 850 hPa wind speeds (Figure 6E) may be the driving force behind high  $\text{SO}_2$ . Comparing wind speeds and  $\text{SO}_2$  concentrations, there are clear indications that wind speed influences  $\text{SO}_2$  concentrations. The wind that is needed to displace the  $\text{SO}_2$  out of the region, over the ocean, has decreased, allowing for  $\text{SO}_2$  concentrations to build over the NCP. The 850 hPa relative humidity values (Figure 6D) are also increasing. Though these values are increasing, we cannot say for certain this should be the case. We assume that since the air is relatively dry, less than 50% in the top 10% mean concentration and the climatological conditions,

the process of absorption of SO<sub>2</sub> by wet deposition is most likely not taking place. The 850 hPa temperatures (Figure 6F) show that increases with temperature will lead to higher SO<sub>2</sub> concentrations. Though one meteorological conditions is not the main source of higher or lower SO<sub>2</sub> concentrations, the interactions with each other can contribute to either.

#### *4.3 Sensitivity analysis of meteorological impact on SO<sub>2</sub>*

GEOS-Chem simulations are conducted for winters of 2009, 2012 and 2013 with a 100% default emission (Figure 7-10). We define 2009 as a low SO<sub>2</sub> year, 2012 as a high year and 2013 intermediate year. These definitions are based on our results found in Figure 2. Regardless of the year, a large area of SO<sub>2</sub> concentration, greater than 2.0 DU, is located over the Shanxi province (Figure 7A-C). However, in 2012 and 2013, this area extends northeastward into the Hebei province and south and southwestward into the Shaanxi, Henan, Hubei and Chongqing provinces. Overall, the model-simulated distribution of SO<sub>2</sub> is consistent with what OMI observed in Figure 2, showing overall low SO<sub>2</sub> amounts in 2009. However, a direct comparison between model and OMI SO<sub>2</sub> amount needs the consideration of other factors such as spatial and temporal sampling characteristics of OMI as well as the averaging kernel used in the OMI SO<sub>2</sub> retrievals (Lee et al. 2009). Overall, past studies have shown GEOS-Chem has a high fidelity in simulating the distribution and transport of SO<sub>2</sub>, and we refer readers to the work by Wang et al. (2012) and references therein. Our aim here is to use the GEOS-Chem model results to assess the meteorological impacts on SO<sub>2</sub>.

Within each year, the variability of columnar SO<sub>2</sub> in winter (quantified as standard deviation in Figure 7D-F) is normally less than 1.5 DU, with larger values corresponding



to the large values of columnar SO<sub>2</sub> itself. However, this correspondence is not linear; contrast between means (Figure 7A-C) and standard deviations (Figure 7D-F) show that locations with largest variability is indeed on the border between Hebei and Shanxi provinces, closer to the edge of the highest SO<sub>2</sub> concentrations. The regions with large relative variability (or standard deviation divided by mean, Figure 7G-I) are those regions that do not have SO<sub>2</sub> sources, nevertheless are affected by the transport of SO<sub>2</sub> from the source region. Overall, in regions with large mean SO<sub>2</sub>, the relative variability is often within 40%, which contrasts with those downwind regions where relative variability is larger than 60%.

To gain insights about possible ranges of SO<sub>2</sub> amounts with respect to the means, Figure 7J-K show the difference between maximum and minimum SO<sub>2</sub> amounts divided by the mean at each grid cell for winters of 2009 and 2012 respectively. The pattern is similar to relative variability (Figure 7G-H), indicating at high SO<sub>2</sub> regions with a possible range of less than 300% and low SO<sub>2</sub> regions with a possible range of larger than 350%. The range of SO<sub>2</sub> change appears to be smaller in 2012 than in 2009.

Change of meteorological conditions in different years can yield a change of winter-mean SO<sub>2</sub> amounts at different locations within  $\pm 20\%$ , as shown in Figure 7L. Further comparison of frequency of columnar SO<sub>2</sub> amount in winters of different years shown significant differences (Figure 9A-C). For example, the data points of SO<sub>2</sub> amounts of less than 1.0 DU show the largest frequency (51.1%) in 2009, while the least frequency (47.2%) in 2013. In comparison, the data points of SO<sub>2</sub> amounts larger than 3 DU show the largest frequency (3.4%) in 2012 and comparable frequency (2.7%) in 2009 and (2.6%) in 2013.

Figure 8 presents the similar analysis as Figure 7, however, for SO<sub>2</sub> amounts in the surface model layer (~100 m). While the distribution of surface SO<sub>2</sub> amounts resembles that of columnar SO<sub>2</sub> amounts, significant differences also are evident. In particular, surface SO<sub>2</sub> amounts are found to be largest in 2009 (Figure 8 A vs. B and C), which contrasts with the columnar amount that is smallest in 2009 (Figure 7 A vs. B and C). In terms of variability (Figure 8D-F), the surface SO<sub>2</sub> amounts are within 0.25 DU and are smaller than its counterparts in the column, and hence the geographic distribution appears to be similar; comparable findings hold for relative variability (Figure 8G-I) and relative range of change (Figure 8J-K). However, the mean of surface SO<sub>2</sub> appears to be more sensitive to the year-to-year change of meteorological conditions and can be up to  $\pm 60\%$  (Figure 8L), a factor of three larger than the counterparts of columnar SO<sub>2</sub> amount (Figure 7L).

The distribution of surface SO<sub>2</sub> amount frequencies, shown in Figure 9D-F for winters of 2009, 2012, and 2013, further reveal that winter 2009 is indeed equally polluted as 2013, with 41.4% of data points in the range of larger than 0.2 DU in the surface layer. In comparison, the winter of 2012 is less polluted with 39.3% of data points for SO<sub>2</sub> amount larger than 0.2 DU. The contrast between Figure 9A-C (showing most polluted in 2012 and least amount in 2013 in terms of relative percentage of data points with values larger than 2 DU) and Figure 9D-F (showing 2012 being less polluted) reveals that the columnar SO<sub>2</sub> may not be representative of surface SO<sub>2</sub> amount, highlighting the importance of meteorological conditions in regulating the vertical profile SO<sub>2</sub>, suggesting complications of using satellite-based columnar SO<sub>2</sub> to characterize the SO<sub>2</sub> air quality at the surface.

Further investigation of the effect of changing SO<sub>2</sub> emission on atmospheric SO<sub>2</sub> distribution is conducted by reducing the GEOS-Chem default SO<sub>2</sub> emission by 50% and then running GEOS-Chem for 2009, 2012, and 2013 (Figure 10). It reveals that for each winter, the response of the seasonal mean columnar SO<sub>2</sub> amount to the reduction of SO<sub>2</sub> emission exhibits similar spatial distributions, regardless of the difference in meteorological conditions; the response, quantified in terms of relative change with respect to the mean without SO<sub>2</sub> emission reduction, appears to be semi-linear with a range of 45 – 55%. Indeed, in the high SO<sub>2</sub> emission regions (in Hebei, Tanjing, and Beijing), the relative change of atmospheric SO<sub>2</sub> columnar amounts is 50%, an nearly exact linear response to the 50% reduction of SO<sub>2</sub> emission. To the south of the high SO<sub>2</sub> emission regions, the SO<sub>2</sub> relative changes range from 50-54%, indicating that the reduction of SO<sub>2</sub> emissions can lead to somewhat in proportionally larger reductions (up to 4%) in atmospheric SO<sub>2</sub> total amount. In contrast, over the northern regions, the SO<sub>2</sub> relative change range is 46%-50%, indicating that atmospheric chemistry can suppress the effect of the reduction of SO<sub>2</sub> emission by up to 4%. Overall, as a whole, the total amount of SO<sub>2</sub> in the atmosphere appears to be a linear response to the change of SO<sub>2</sub> emission, at least in the seasonal averages.

Further analysis, however, shows that the response of surface SO<sub>2</sub> amounts are highly nonlinear with respect to the change of SO<sub>2</sub> emissions (Figure 10C-E). For a 50% reduction of emission, the response is in the range of 20-80% and exhibits different spatial distributions in different years (Figure 10C-E). In high SO<sub>2</sub> emission regions, the reduction of 50% emission leads to a 30% reduction of atmospheric SO<sub>2</sub> near the surface in 2009, however, a 70% reduction in 2012, and nearly 50% in 2013 (Figure 10C-E

respectively). Depending on the region, the year-to-year change of meteorological conditions can result up to  $\pm 50\%$  variability in the response (or relative change, Figure 10F-H). It is interesting to note that in all three years, reduction of emissions appears to in proportionally suppressing the more extreme polluted cases; for near-surface  $\text{SO}_2$  amounts larger than 0.4 DU (in simulations with 100% emission), the corresponding portion of data points are 9.1% 8.1% and 9.3% in 2009, 2012, and 2013 respectively, which are all higher than their counterparts in the simulation with 50% emission (e.g. 8.9%, 8% and 8.8% of data points with  $\text{SO}_2$  values larger than 0.2 DU).

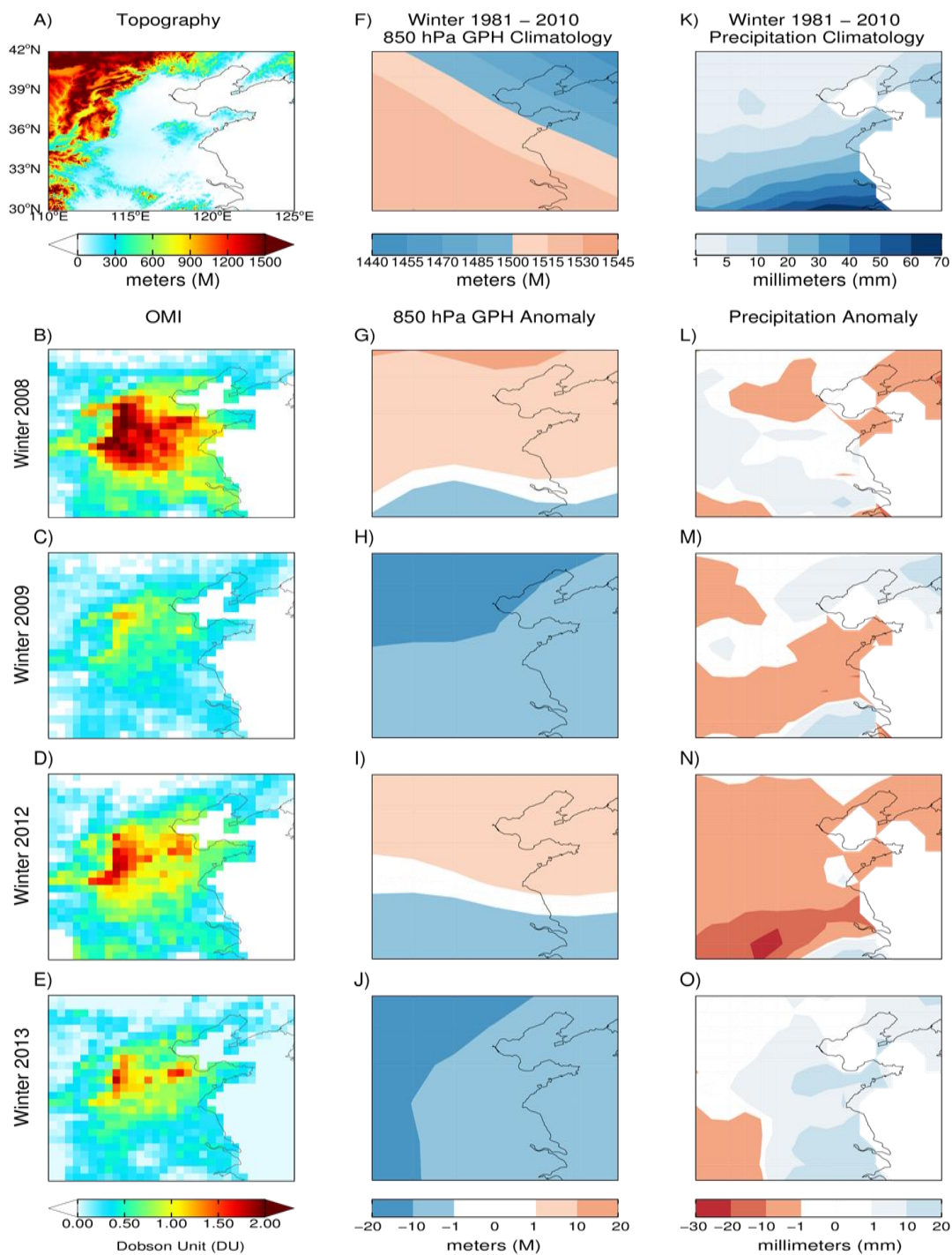


Figure 2. For comparison purposes the topography of the North China Plain (A), winter climatology (1981-2010) of heights at 850 hPa (F) and precipitation (K) are shown at top. Also shown are the winter average for OMI (B-E), GPH anomaly (G-J) and precipitation anomaly (L-O) for the winters of 2008 (second row from the top), 2009 (third row), 2012 (fourth row) and 2013 (fifth row).

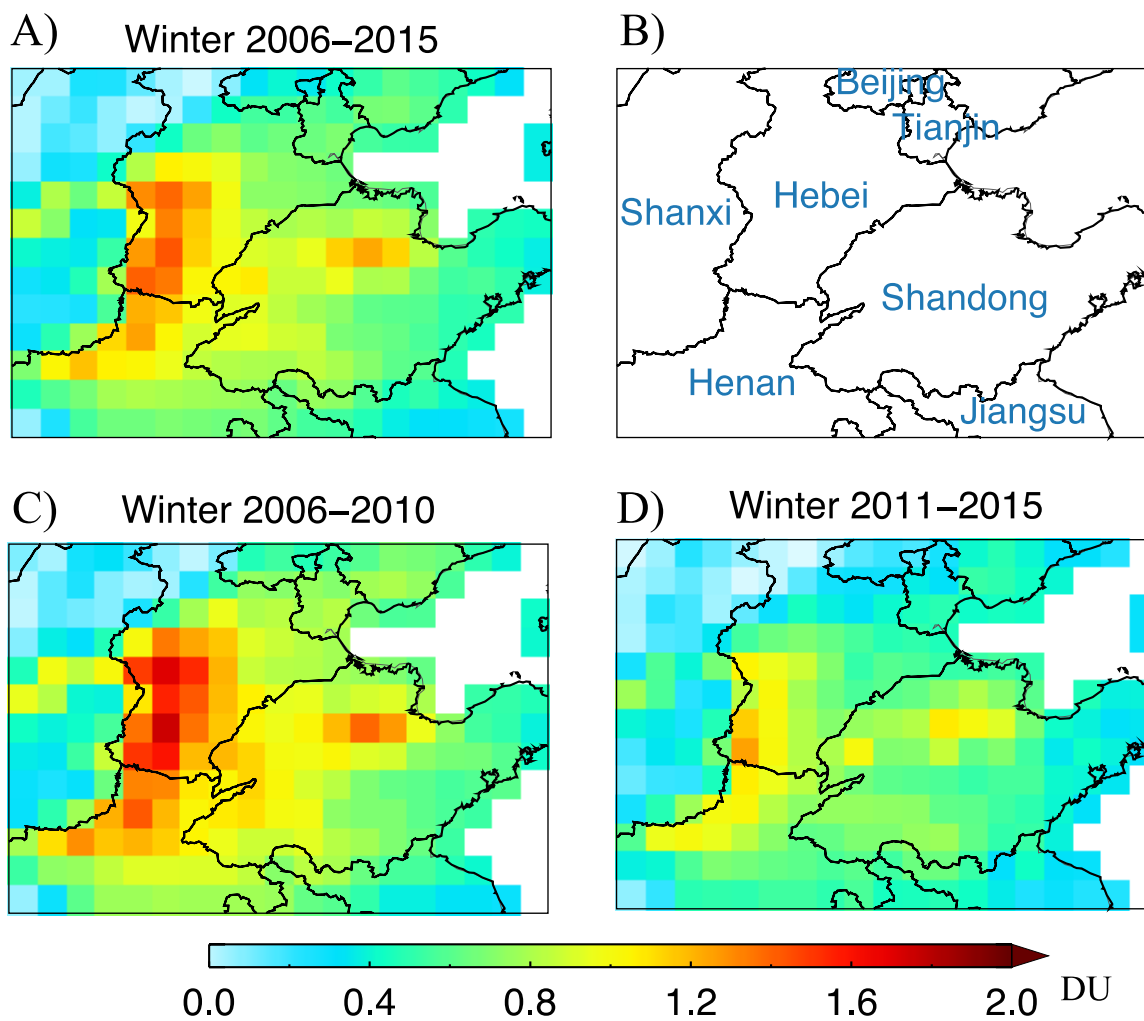


Figure 3. Average OMI SO<sub>2</sub> amount for winters (A) 2006-2015, (C) 2006-2010, and (D) 2011-2015 re-gridded to 0.5°x0.5°. (B) shows the map of different Chinese provinces in the study region.

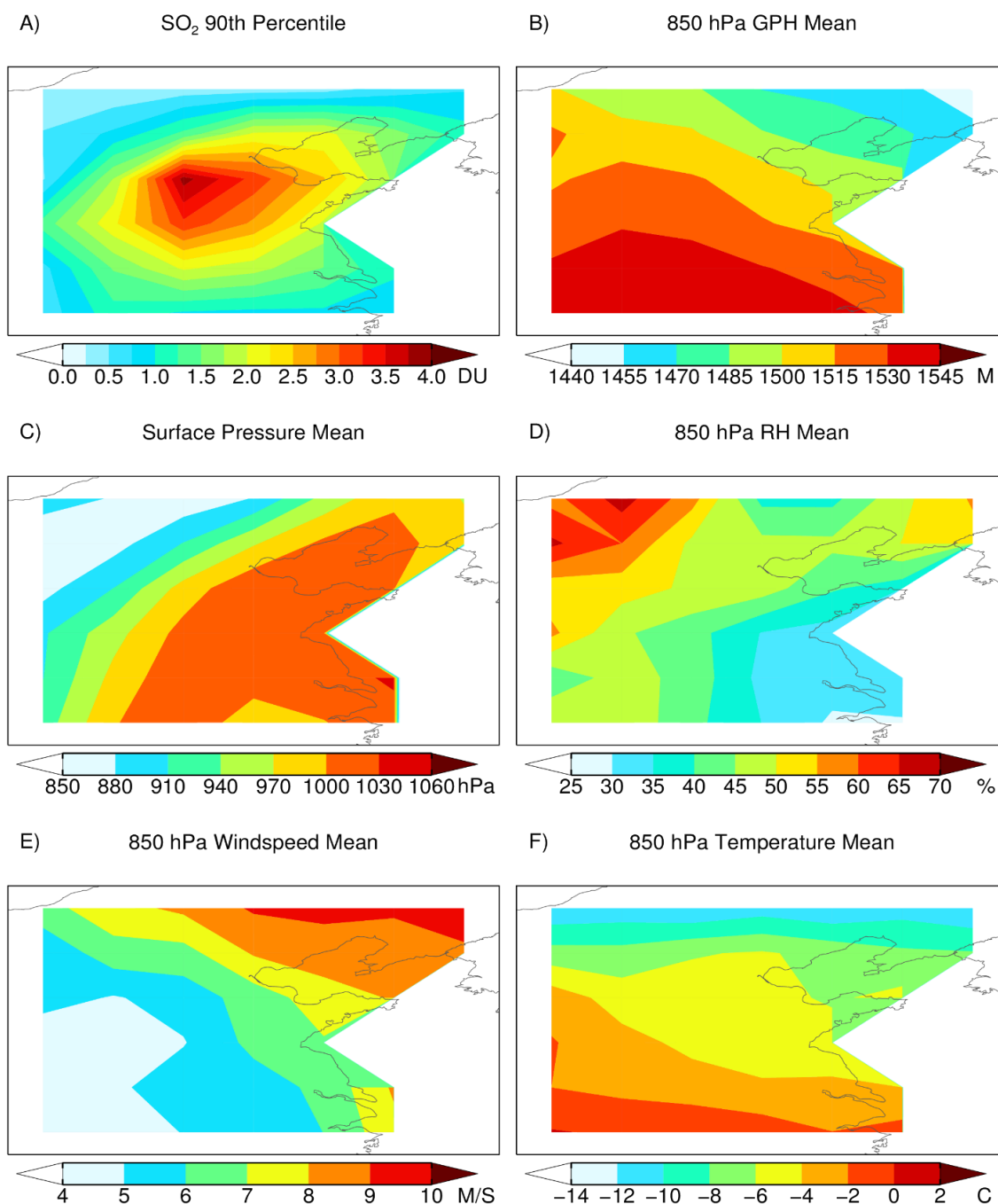


Figure 4. (A) spatial distribution of the average of top 10% of OMI SO<sub>2</sub> amounts for each 2.5°×2.5° grid box during winters of 2006 – 2015. (B)-(F) is similar to (A), but for each grid box, respectively show the average of geopotential height (GPH, in meter) at 850 hPa, surface pressure (in hPa), and 850 hPa relative humidity, wind speed, and temperature data corresponding to the days that have the top 10% SO<sub>2</sub> amount for that grid box.

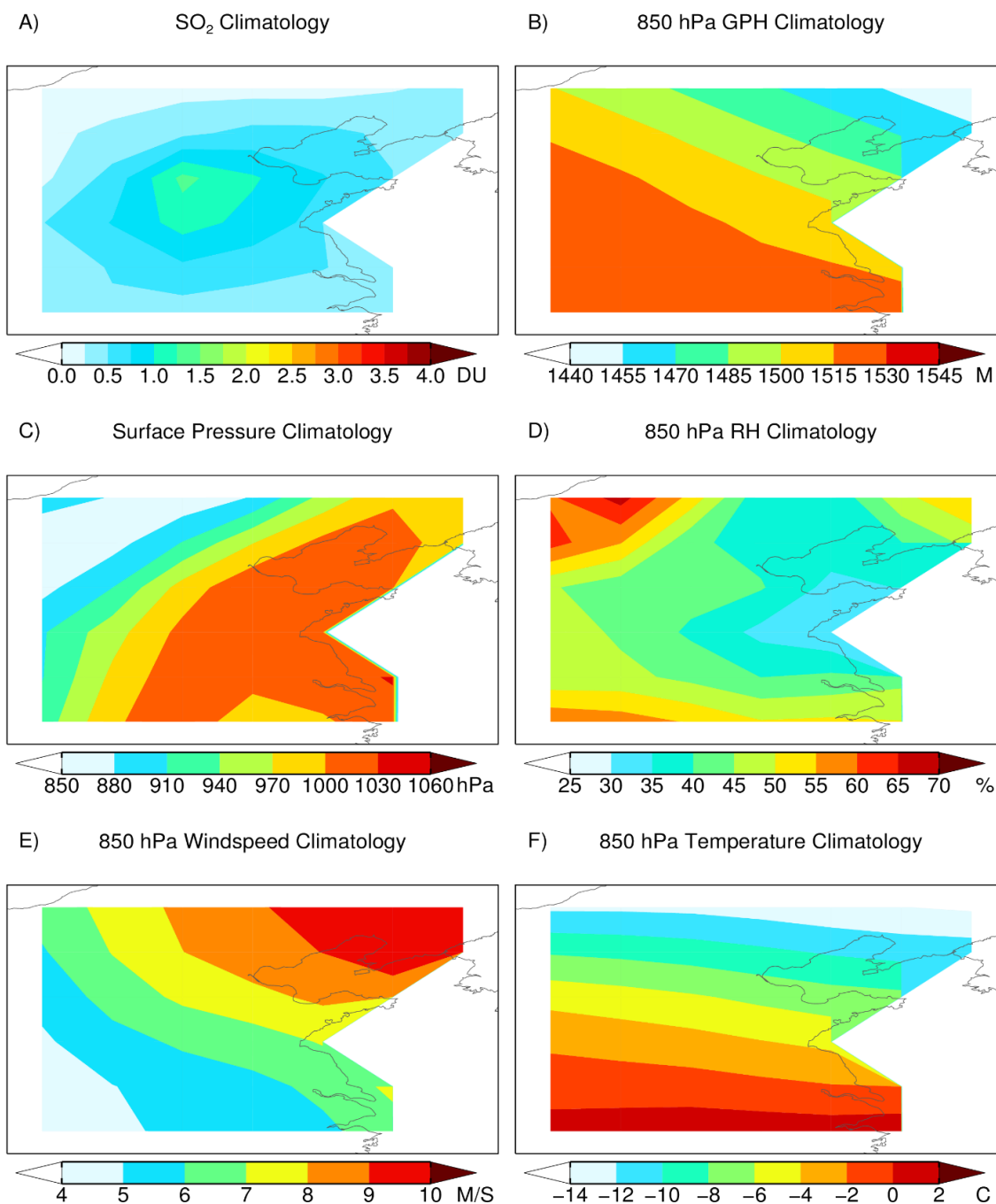


Figure 5. Similar as Figure 4, but shows the climatology or the average of variables for each  $2.5^\circ \times 2.5^\circ$  grid box in all winter days that have valid data for the corresponding variable during 2006-2015.



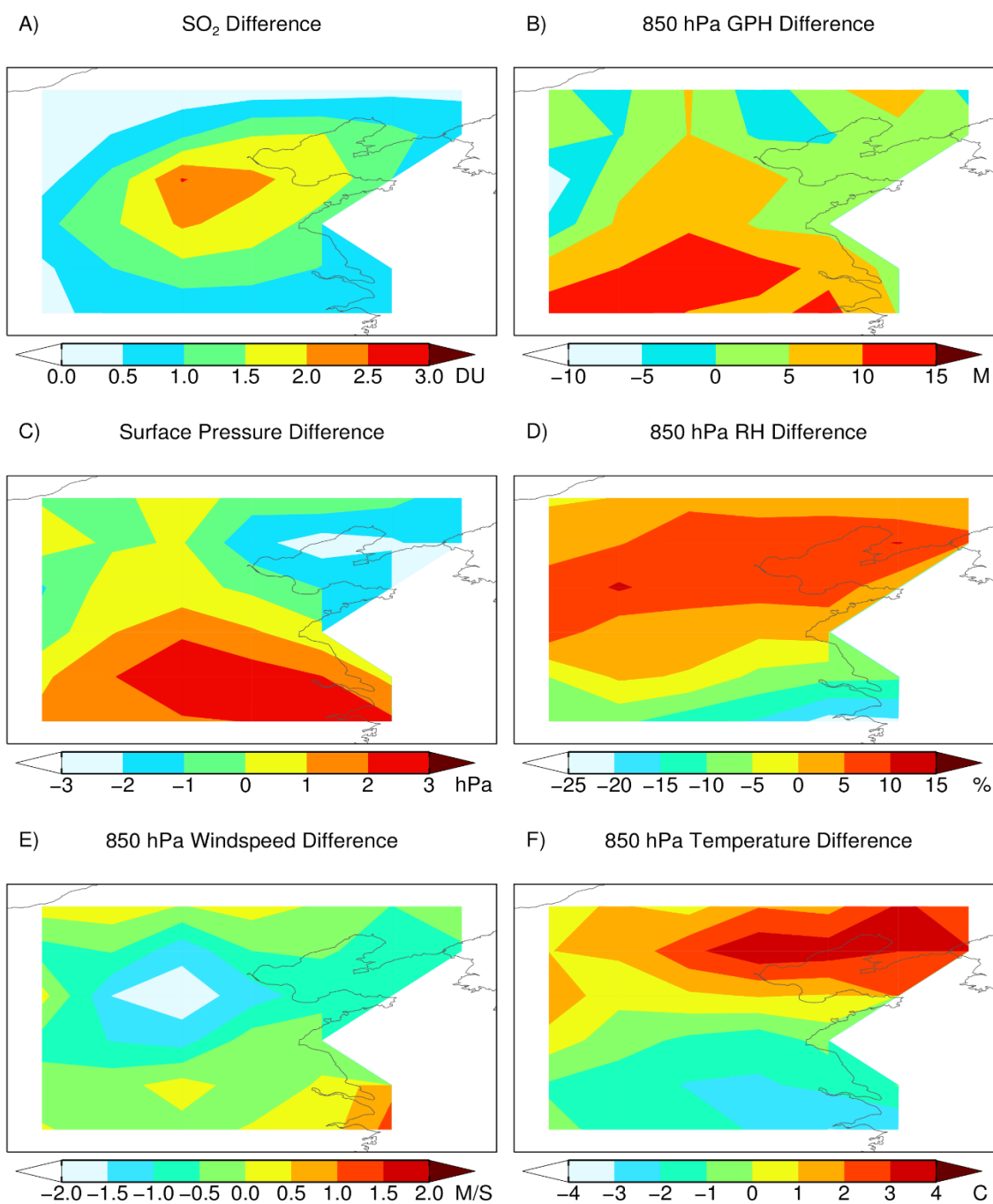


Figure 6. Same as Figure 4 but shows the difference between Figure 4 and Figure 5.

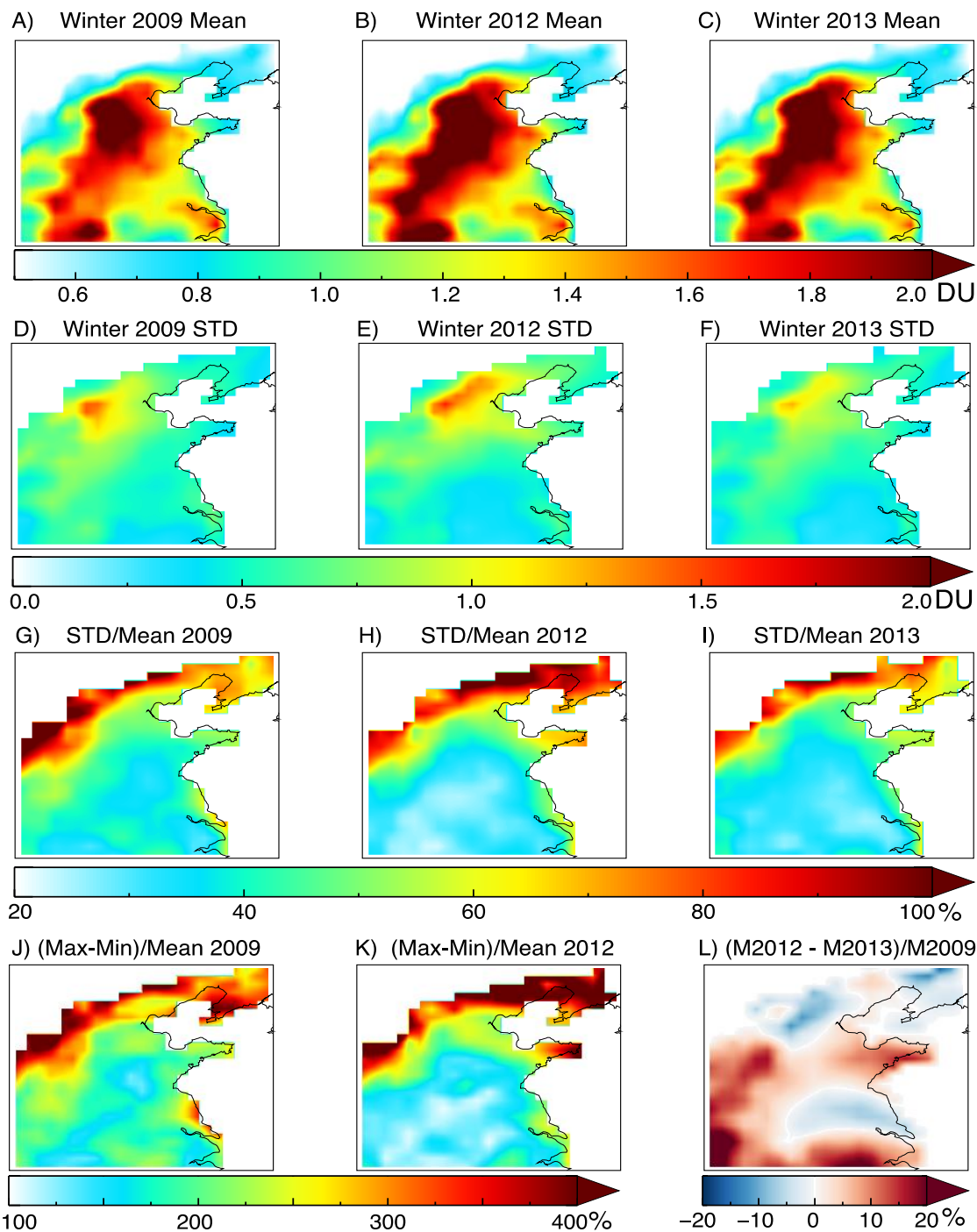


Figure 7. A-C: Mean of columnar SO<sub>2</sub> amounts simulated by GEOS-Chem for the winters of 2009, 2012 and 2013, respectively. D-F: similar as A-C, however, for standard deviation. G-I: similar as D-F, however, for relative variation (standard deviation with respect to the mean). J-K: the range of SO<sub>2</sub> with respect to the mean for winters of 2009 and 2012, respectively. L: change of mean SO<sub>2</sub> between 2012 and 2013 with respect to the mean of 2009.

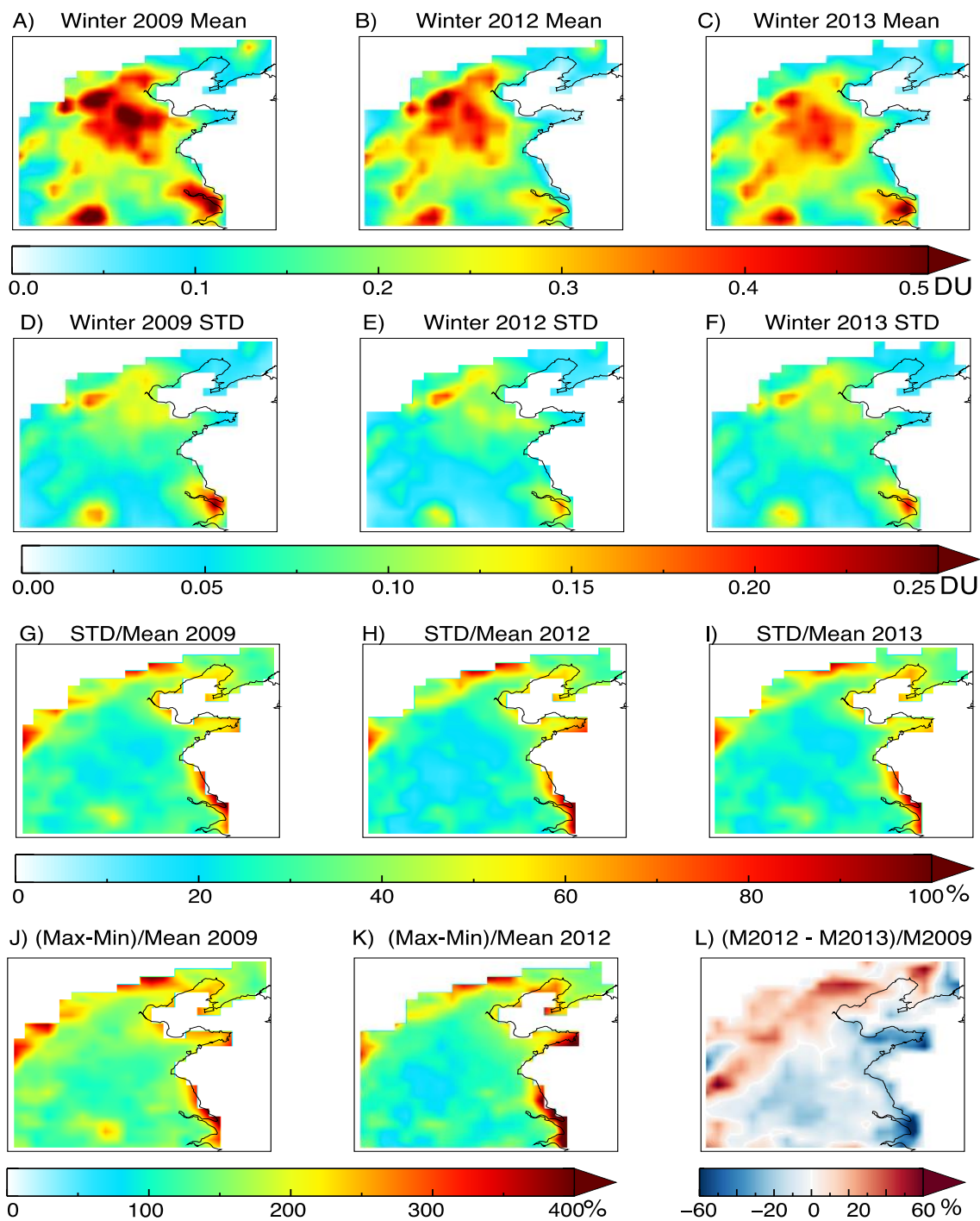


Figure 8. Same as Figure 7, but for SO<sub>2</sub> amount in the surface layer of the model.

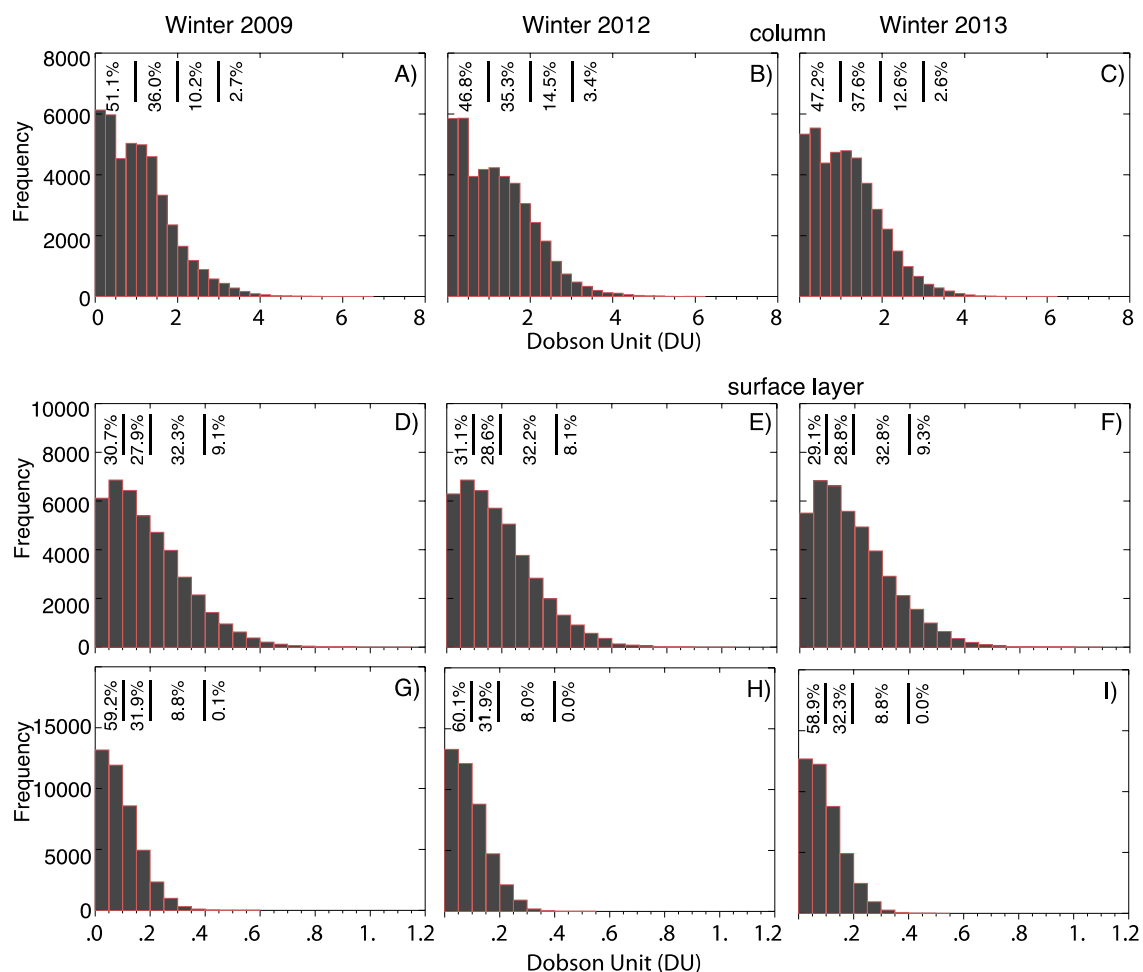
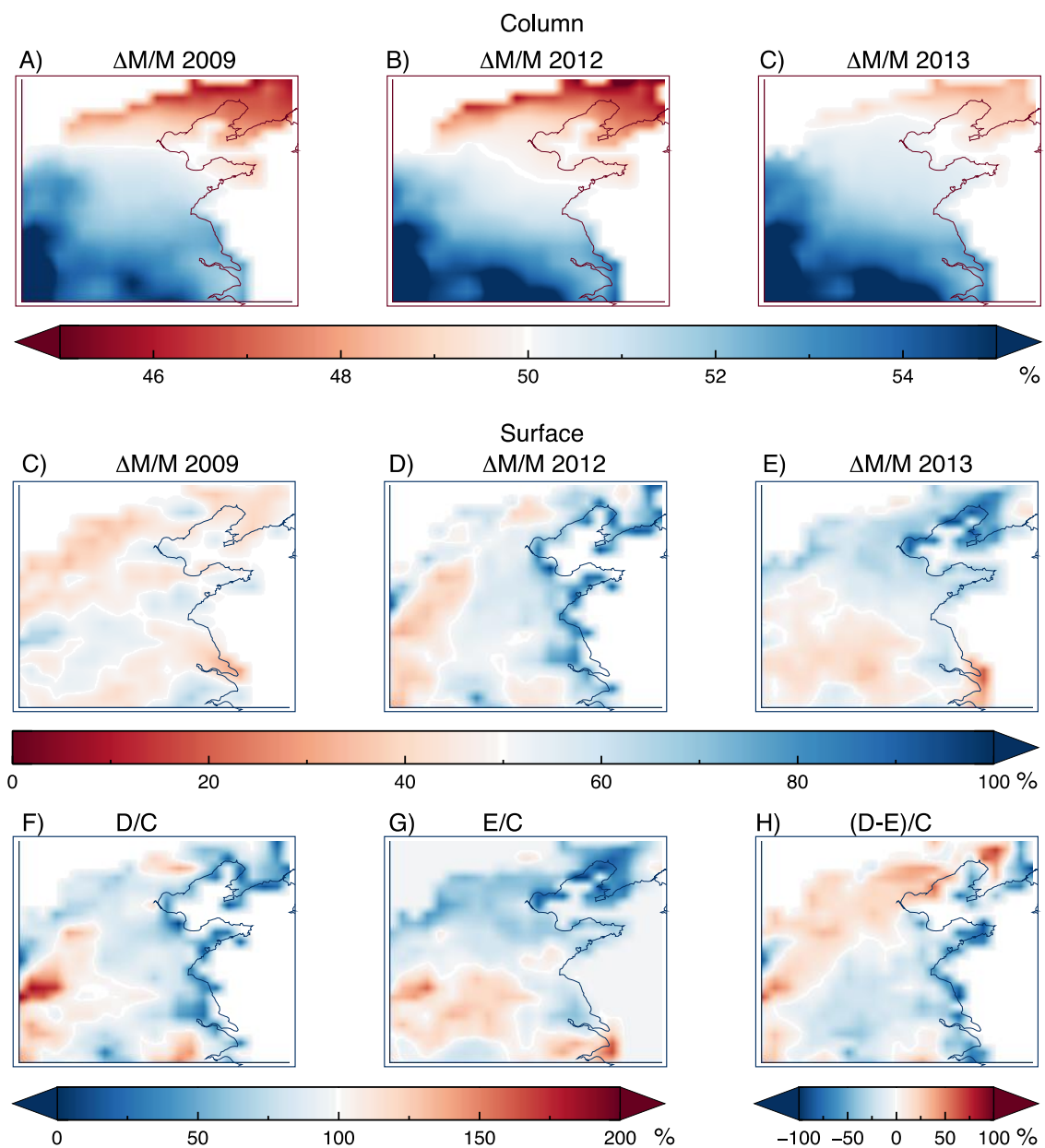


Figure 9. Frequency of GEOS-Chem simulated hourly columnar (top row) and surface layer (middle row) SO<sub>2</sub> amounts at each model grid box over the continent in the model domain for 2009 (left column), 2012 (middle column), and 2013 (right column), respectively. The bottom row is for surface layer SO<sub>2</sub> amounts simulated by GEOS-Chem with a 50% reduction of SO<sub>2</sub> emission. The relative percentages of the number of data points at every 1 DU interval up to 3 DU and more than 3 DU are shown on the top left of each panel in the top row, and the relative percentages of the number of data points in range of 0 – 0.1 DU, 0.1 – 0.2 DU, 0.2 – 0.4 DU, and more than 0.4 DU are shown on the top left of each panel in middle and bottom row.



Figures 10. Relative change of winter mean (M) SO<sub>2</sub> amounts ( $\Delta M/M$ ) in response to the 50% reduction SO<sub>2</sub> emission for 2009, 2012 and 2013 respectively. Top row shows the relative change for columnar SO<sub>2</sub> amounts while the second row from the top for SO<sub>2</sub> amounts at the surface. F and G show the ratio of relative change in 2009 and 2013 with respect to the counterpart in 2012 (e.g., data values in panel D and E divided by panel C), respectively. H shows the ratio of difference of relative change between 2012 and 2009 with respect to relative change in 2012. Lines in white color show the isopleths at 0%, 50%, and 100% for A-E, F-G, and H, respectively.

## 5. Summary

Using OMI and GEOS-Chem, we studied the characteristics of how meteorological conditions affect SO<sub>2</sub> distributions in the NCP during the winters of 2006-2015. The main conclusions are as follows:

- OMI SO<sub>2</sub> data show that atmospheric SO<sub>2</sub> concentrations in China have drastically decreased by 30% from the 2006-2010 period to the 2011- 2015 period. This can be attributed to the installation of flue-gas desulfurization devices.
- High SO<sub>2</sub> days are found to be associated with the stagnant, warm, and moist air masses that average 1-2 hPa higher in surface pressure, as well as 850 hPa level increases in geopotential height of 5-10 m, 1-3 °C warmer temperatures, 10%-15% higher relative humidities, and up to 2 m s<sup>-1</sup> slower wind speeds.
- Numerical experiments with GEOS-Chem model simulations reveal that the relative change of columnar distribution of SO<sub>2</sub> in response to a change of meteorological conditions and seasonal averaged emissions are normally within 10%-20%, suggesting a high consistence or semi-linear relationship between columnar SO<sub>2</sub> observations and SO<sub>2</sub> emissions are expected. In contrast, the relative change of SO<sub>2</sub> amounts near the surface exhibit stronger dependence on meteorological conditions and a non-linear relationship with respect to the change of emissions; the year-to-year change of surface SO<sub>2</sub> amounts due to change of meteorological conditions can be up to 20-30% and the response to the change of emissions can deviate from linear relationship by up to 50%. It is concluded that

the climatology of columnar SO<sub>2</sub> amounts is not representative and sometime can be opposite to the climatology of surface SO<sub>2</sub> amounts.

These findings underscore the importance of considering the role of meteorological conditions in the application of satellite-based SO<sub>2</sub> data to study air pollution events. When combining meteorological data with satellite-based SO<sub>2</sub> data, an observation-based air pollution climatology can be revealed and studied. However, as OMI's SO<sub>2</sub> data record only starts in 2006 and with limited spatial and temporal sampling due to the row anomaly, a longer SO<sub>2</sub> data record from space with high density in spatial and temporal sampling is needed, and thus would reveal insights from a SO<sub>2</sub> pollution climatology and associated meteorological conditions.

## References

- Afe, O. T., A. Richter, B. Sierk, F. Wittrock, and J. P. Burrows, 2004: BrO emission from volcanoes: A survey using GOME and SCIAMACHY measurements. *Geophys. Res. Lett.*, 31, L24113, doi:10.1029/2004GL020994.
- Bey, I., D. J. Jacob, R. M. Yantosca, J. A. Logan, B. D. Field, A. M. Fiore, Q. Li, H. Y. Liu, L. J. Mickley, and M. G. Schultz, 2001: Global modeling of tropospheric chemistry with assimilated meteorology:: Model description and evaluation. *Journal of Geophysical Research*, 106, 23073-23095, doi:10.1029/2001JD000807.
- Bridgman, H. A., T. D. Davies, T. Jickells, I. Hunova, K. Tovey, K. Bridges, and V. Surapipith, 2002: Air pollution in the Krusne Hory region, Czech Republic during the 1990s. *Atmospheric Environment*, 36, 3375-3389, doi:10.1016/S1352-2310(02)00317-5.
- Carn, S. A., K. Yang, A. J. Prata, and N. A. Krotkov, 2015: Extending the long-term record of volcanic SO<sub>2</sub> emissions with the Ozone Mapping and Profiler Suite nadir mapper. *Geophysical Research Letters*, 42, 925-932, doi:10.1002/2014GL062437.
- Chan, C., K., X. Yao, 2008: Air pollution in mega cities in China. *Atmospheric Environment*, 42, 1-42, doi:10.1016/j.atmosenv.2007.09.003.
- Cuhadaroglu, B., E. Demirci, 1997 Influence of some meteorological factors on air pollution in Trabzon City. *Energy and Buildings*, 3, 179-184.
- Fiore, A. M., et al. (2012), Global air quality and climate, *Chemical Society Reviews*, 41(19), 6663-6683.



- He, H., C. Li, C. P. Loughner, Z. Li, N. A. Krotkov, K. Yang, L. Wang, Y. Zheng, X. Bao, G. Zhao, and R. R. Dickerson, 2012: SO<sub>2</sub> over central China: Measurements, numerical simulations and the tropospheric sulfur budget. *Journal of Geophysical Research*, 16, D00K37, doi:10.1029/2011JD016473.
- Iten, N., A. T. Selici, 2008: Investigating the impacts of some meteorological parameters on air pollution in Balikesir, Turkey. *Environmental Monitoring Assessment*, 140, 267-277.
- Krotkov, N. A., S. A. Carn, A. J. Krueger, P. K. Bhartia, and K. Yang, 2006: Band residual difference algorithm for retrieval of SO<sub>2</sub> from the Aura Ozone Monitoring Instrument (OMI). *IEEE Transactions on Geoscience and Remote Sensing*, 44, 1259-1266, doi:10.1109/TGRS.2005.861932.
- Krotkov, N. A., M. R. Schoeberl, G. A. Morris, S. Carn, and K. Yang, 2010: Dispersion and lifetime of the SO<sub>2</sub> cloud from the August 2008 Kasatochi eruption. *Journal of Geophysical Research*, 115, 1-13, doi:10.1029/2010JD013984.
- Krotkov, N. A., B. McClure, R. R. Dickerson, S. A. Carn, C. Li, P. K. Bhartia, K. Yang, A. J. Krueger, Z. L. Li, P. F. Levelt, H. Chen, P. Wang, and D. Lu, 2008: Validation of SO<sub>2</sub> retrievals from the Ozone Monitoring Instrument over NE China. *Journal of Geophysical Research*, 113, 1-13, doi:10.1029/2007JD008818.
- Lee, C., R. V. Martin, A. van Donkelaar, A. O'Byrne, N. Krotkov, A. Richter, L. G. Huey, and J. S. Holloway, 2009: Retrieval of vertical columns of sulfur dioxide from SCIAMACHY and OMI: Air mass factor algorithm development,

- validation, and error analysis. *Journal of Geophysical Research*, 114, D22303, doi:10.1029/2009JD012123.
- Lee, C., A. Richter, and J. P. Burrows, 2008: SO<sub>2</sub> retrieval from SCIAMACHY using the Weighting Function DOAS (WFDOAS) technique: Comparison with standard DOAS retrieval. *Atmos. Chem. Phys.*, 8, 6137-6145, doi:10.5194/acp-8-6137-2008.
- Lee, C., R. V. Martin, A. v. Donkelarr, H. Lee, R. R. Dickerson, J. C. Hains, N. Krotkov, A. Richter, K. Vinnikov, and J. J. Schwab, 2011: SO<sub>2</sub> emissions and lifetimes: Estimates from inverse modeling using in situ and global, space-based (SCIAMACHY and OMI) observations. *Journal of Geophysical Research*, 116, 1-13, doi:10.1029/2010JD014758.
- Levelt, P. F., van den Oord, Gijsbertus H. J., M. R. Dobber, A. Mälkki, H. Visser, J. d. Vries, P. Stammes, J. O. V. Lundell, and H. Saari, 2006: The Ozone Monitoring Instrument. *IEEE Transactions on Geoscience and Remote Sensing*, 44, 1093-1101.
- Li, C., Q. Zhang, N. A. Krotkov, D. G. Streets, K. He, S.-C. Tsay, and J. F. Gleason, 2010: Recent large reduction in sulfur dioxide emissions from Chinese power plants observed by the Ozone Monitoring Instrument. *Geophysical Research Letters*, 37, L08807
- Lu, Z., Streets, D.G., Zhang, Q., Wang, S., Carmichael, G. R., Cheng, Y.F., Wei, C., Chin, M., Diehl, T., Tan, Q., 2010: Sulfur dioxide emissions in China and sulfur trends in East Asia since 2000. *Atmos. Chem. Phys.*, 10, 6311, doi:10.5194/acp-10-6311-2010.

- Lu, Z., Q. Zhang, and D. G. Streets, 2011: Sulfur dioxide and primary carbonaceous aerosol emissions in China and India, 1996-2010. *Atmos. Chem. Phys.*, 11, 9839-9864, doi:10.5194/acp-11-9839-2011.
- Massie, S. T., O. Torres, and S. J. Smith, 2004: Total Ozone Mapping Spectrometer (TOMS) observations of increases in Asian aerosol in winter from 1979 to 2000. *Journal of Geophysical Research*, 109, 1-14, doi:10.1029/2004JD004620.
- Olivier, J. G. J., J. J. M. Berdowski, 2001: Global emissions sources and sinks. *The Climate System*, , 33-78.
- Park, R. J., D. J. Jacob, B. D. Field, and R. M. Yantosca, 2004: Natural and transboundary pollution influences on sulfate-nitrate-ammonium aerosols in the United States: Implications for policy. *Journal of Geophysical Research*, 109, 1-20, doi:10.1029/2003JD004473.
- Richter, A., F. Wittrock, and J. P. Burrows (2006), SO<sub>2</sub> Measurements with SCIAMACHY, in Proceeding of Atmospheric Science Conference, Frascati, Italy, 8–12 May, *ESA Publ. SP-628*, ESA/ESRIN, Noordwijk, Netherlands.
- Smith, S. J., J. van Aardenne, Z. Klimont, R. J. Andres, A. Volke, and S. Delgado Arias, 2011: Anthropogenic sulfur dioxide emissions: 1850-2005. *Atmos. Chem. Phys.*, 11, 1101-1116, doi:10.5194/acp-11-1101-2011.
- Wang, J., S. Park, J. Zeng, C. Ge, K. Yang, S. Carn, N. Krotkov, and A. H. Omar, 2013: Modeling of 2008 Kasatochi volcanic sulfate direct radiative forcing: assimilation of OMI SO<sub>2</sub> plume height data and comparison with MODIS and CALIOP

- observations. *Atmos. Chem. Phys.*, 13, 1895-1912, doi:10.5194/acp-13-1895-2013.
- WHO, 2001: Environment and People's Health in China. [Available online at [http://www.wpro.who.int/environmental\\_health/documents/docs/CHNEnvironmentalHealth.pdf](http://www.wpro.who.int/environmental_health/documents/docs/CHNEnvironmentalHealth.pdf)].
- Xue, D., J. Yin, 2013: Meteorological influence on predicting surface SO<sub>2</sub> concentration from satellite remote sensing in Shanghai, China. *Environmental Monitoring Assessment*, 186, 2895-2906, doi:10.1007/s10661-013-3588-2.
- Yang, K., N. A. Krotkov, A. J. Krueger, S. A. Carn, P. K. Bhartia, and P. F. Levelt, 2007: Retrieval of large volcanic SO<sub>2</sub> columns from the Aura Ozone Monitoring Instrument: Comparison and limitations. *Journal of Geophysical Research*, 112, D24S43, doi:10.1029/2007JD008825.
- Yang, K., R. Dickerson, S. Carn, J. Wang, and C. Ge, 2013: First Observations of SO<sub>2</sub> from Suomi NPP OMPS: Widespread Air Pollution Events over China. *Geophysical Research Letters*, 40, 4957-4962, doi:10.1002/grl.50952.
- Zhang, Q. Q., Y. Yang, Q. Ma, Y. Yao, Y. Xie, and K. He, 2015: Regional differences in Chinese SO<sub>2</sub> emission control efficiency and policy implications. *Atmos. Chem. Phys.*, 15, 6521-6533, doi:10.5194/acp-15-6521-2015.
- Zhang, Q., D. G. Streets, G. R. Carmichael, K. B. He, H. Huo, A. Kannari, Z. Klimont, I. S. Park, S. Reddy, J. S. Fu, D. Chen, L. Duan, Y. Lei, L. T. Wang, and Z. L. Yao, 2009: Asian emissions in 2006 for the NASA INTEX-B mission. *Atmospheric Chemistry and Physics*, 9, 5131-5153.

Zhang, X., J. van Geffen, H. Liao, P. Zhang, and S. Lou, 2012: Spatiotemporal variations of tropospheric SO<sub>2</sub> over China by SCIAMACHY observations during 2004–2009. *Atmospheric Environment*, 60, 238-246, doi:10.1016/j.atmosenv.2012.06.009.